# Journal Pre-proof

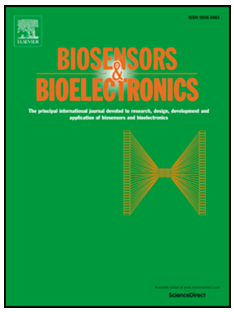


A facile thermometer-like electrophoresis titration biosensor for alternative miRNA assay via moving reaction boundary chip

Ling Chen, Qiang Zhang, Weiwen Liu, Hua Xiao, Xiaoping Liu, Liuyin Fan, Yuxing Wang, Honggen Li, Chengxi Cao

PII: S0956-5663(20)30665-5

DOI: https://doi.org/10.1016/j.bios.2020.112676

Reference: BIOS 112676

To appear in: *Biosensors and Bioelectronics*

Received Date: 11 August 2020

Revised Date: 14 September 2020

Accepted Date: 1 October 2020

Please cite this article as:

## Credit authorship contribution statement

**Ling Chen:** Conceptualization, Data curation, Formal analysis, Investigation, Methodology, Draft organization. **Qiang Zhang:** Methodology, Writing - review & editing. **Weiwen Liu:** Writing - review & editing. **Hua Xiao:** Resources. **Xiaoping Liu:** chip design & fabrication. **Liuyin Fan:** Validation. **Yuxing Wang:** Validation. **Honggen Li:** Device, Validation, Funding asistance. **Chengxi Cao:** Conceptualization, Funding acquisition, Investigation, Methodology, Project administration, Writing-review & editing.

# A facile thermometer-like electrophoresis titration biosensor for alternative miRNA assay via moving reaction boundary chip

Ling Chen[a,c,#], Qiang Zhang[a,#], Weiwen Liu[a], Hua Xiao[c], Xiaoping Liu[a], Liuyin Fan[d], Yuxing Wang[b], Honggen Li[b,**], and Chengxi Cao[a,c*1]

[a] *Department of Instrument Science and Engineering, School of Electronic Information & Electrical Engineering, Shanghai Jiao Tong University, Shanghai 200240, China*

[b] *School of Physics and Astronomy, Shanghai Jiao Tong University, Shanghai 200240, China*

[c] *School of Life Science and Biotechnology, State Key Laboratory of Microbial Metabolism, Shanghai Jiao Tong University, Shanghai 200240, China*

[d] *Student Innovation Center, Shanghai Jiao Tong University, Shanghai 200240, China*

**Herein, a facile thermometer-like model of electrophoresis titration (ET) biosensor was proposed as an alternative tool for miRNA assay via moving reaction boundary (MRB) chip. For proof-of-concept demonstration, miRNA-122 and catalyzed hairpin assembly (CHA) were chosen as the model analyte and amplification, respectively. In the developed ET system, miRNA triggered the CHA with two hairpin probes (H1, H2) to yield H1-H2 duplexes with negative charges. Under an electric field, the duplexes moved into ET channel, and neutralized the acidic TAE buffer creating an MRB indicated by SYBR Green I (SGI). The model revealed that the MRB distance was as a function of logarithmic miRNA-122 content, indicating a facile sensing model. The relevant experiments were conducted and systemically validated the model of miRNA ET. Under the optimized conditions, the linear range of ET sensor was from 20 fM to 1 nM and the limit of detection (LOD) was 10 fM, showing a more than 100-fold sensitive increase in contrast to the one with a single CHA amplification. The mechanism of sensitive increase was well unveiled by the designed experiments. In addition, the ET biosensor had good selectivity, stability (less than 5% for intra-day and inter-day) and recovery (96%~110%), and was successfully applied for the assay of miRNA-122 and miRNA let-7a in real bio-fluids of serum and cancer cell lysate. Evidently, the proposed biosensor might be used as an alternative assay tool after nucleic acid amplification due to its high simplicity, sensitivity, specificity, linearity, stability and recovery.**

**Keywords:** Biosensor; Catalyzed hairpin assembly; Electrophoresis titration chip; MicroRNA; Moving reaction boundary

## 1. Introduction

MicroRNAs (miRNAs) are a class of small and noncoding single-stranded RNA molecules with 18-25 nucleotides (He et al., 2005; Ventura and Jacks, 2009; Necsulea et al., 2014; Ha et al., 2014). They serve as

[1]The first and second correspondence authors: *Dr. Chengxi Cao (email address: cxcao@sjtu.edu.cn), and **Dr. Honggen Li (email address: lihonggen@sjtu.edu.cn).

[#]The first two authors have equal contribution to the work.

endogenous gene regulators by inhibiting translational expression or affecting on themselves degradations, and play key roles in many biological processes, e.g., gene expression, cell proliferation, cell differentiation, and cell apoptosis (Kawasaki and Taira, 2003; Xiao et al., 2009; Nicoloso et al., 2009; Wen et al., 2012; Li et al., 2016; Rafiee-Pour et al., 2016). Particularly, an abnormal expression of miRNAs is closely associated with various diseases, hence many miRNAs become valuable diagnostic markers and therapeutic targets for several cancers, scleroderma and cardiovascular diseases (Hwang et al., 2006; Bartel, 2009; Brase et al., 2010; Zhu et al., 2013; Zhong et al., 2014; Tao et al., 2016).

Many efforts have been made to develop the analytical method of miRNA in the last decade. These methods concerned the northern blotting (Pall et al., 2007), the reverse transcription polymerase chain reaction (RT-PCR) (Li et al., 2009), and the microarray analyses (Lee et al., 2010) as well as the next generation sequencing (Bhattacharya et al., 2019). In addition, numerous isothermal amplification methods (Huang et al., 2012; Chen et al., 2013) have been developed, such as the hybridization chain reaction (HCR) amplification (Yang et al., 2015), the catalyzed hairpin assembly (CHA) amplification (Liu et al., 2013; Zhang et al., 2017), the rolling circle amplification (RCA) (Ge et al., 2014) and the isothermal exponential amplification (Yu et al., 2014).

At the same time, the detection techniques have been used for the bioassay of miRNA amplification product. They included the fluorescence intensity assay (Ding et al., 2018; Li et al., 2018), ratiometric fluorescence assay (Fang et al., 2018), fluorescence anisotropy analysis (Zhen et al., 2017), electrochemical sensing (Zhang et al., 2017), chemiluminescent intensity (Li et al., 2016), and separation of gel electrophoresis with fluorescence staining and miRNA band scanning (Lee et al., 2014; Lee et al., 2015; Dai et al., 2018; Zhang et al., 2018). However, rare work was reported on a facile thermometer-like biosensor of miRNA in bio-fluids.

The issue might be well addressed by the concept of electrophoresis titration (ET) biosensor evolved from the model of moving reaction boundary (MRB) (Deman, 1970; Deman, 1970; Cao, 1998; Cao et al., 2005). In the last five years, several ET techniques have been proposed, including the ET sensing of protein content in milk (Zhang et al., 2016; Wang et al., 2019), the highly effective ET analysis of enzyme (Cao et al., 2018), and the real chip ELISA (Kong et al., 2019). In those ETs, the target analyte was indirectly transferred as a positive/negative reactive ion, by designing a negative/positive reactive ion a visual ET sensing was created between the positive/negative and negative/positive reaction ionic pairs (e.g., $H^+$ and

$OH^-$). Thus, the target analyte could be assayed via the visual ET sensor. Whereas, the concept of ET was rarely used for designing a facile thermometer-like biosensor for assay of miRNA to the authors' knowledge.

Herein, a facile thermometer-like model of miRNA ET biosensor was proposed based on the MRB chip. For the proof-of-concept demonstration, CHA was used as a model miRNA amplification due to its label-free non-enzymatic reaction, and miRNA-122 was chosen as a model analyte thanks to its valuable diagnostic marker and therapeutic target for hepatocellular carcinoma and liver injury (Mariana et al., 2002; Howell et al., 2018; Ahmed et al., 2018; Liao et al., 2020). The experiments revealed that: (i) the MRB distance was as a function of logarithmic miRNA-122 content, implying a facile thermometer-like sensing; (ii) the LOD of ET was as low as 10 fM, showing more than 100-fold sensitive increase in contrast to the one with a single CHA; and (iii) the ET had high selectivity. To the best of our knowledge, this was the first work reporting a thermometer-like miRNA ET sensing via an MRB chip.

# 2. Material and methods

## 2.1. Materials

All of the oligonucleotides used in this work were obtained from Sangon Biotechnology Co. Ltd. (Shanghai, China) and were high-performance liquid chromatography (HPLC) purified by the manufacturer. The sequences of these miRNAs and DNA probes were given in **Table S1**. 2-amino-2-(hydroxymethyl)-1,3-propanediol (Tris) and ethyl-enediaminetetra acetic acid (EDTA) were bought from Sigma Aldrich Co. (Shanghai, China). Agarose gel, sodium hydroxide, hydrochloric acid, boric acid, acetic acid and potassium chloride were bought from Sinopharm Chemical Reagent Co. Ltd. (Beijing, China). TRIzol reagent, SYBR Green I, DNA marker (25-500 bp) and diethylpyro-carbonate (DEPC)-treated water were purchased from Sangon Biotechnology Co. Ltd. (Shanghai, China). DEPC-treated deionized water was used in all experiments to protect all miRNAs from RNase degradation. Graphene oxide (~5 μm in width × 2-10 nm in thickness, 4 mg/mL) was purchased from Bailingwei Chemical Technology Co. Ltd. (Shanghai, China). All reagents were analytical grade and used without further purification. Ultrapure water (less than 0.055 μS $cm^{-1}$) was obtained via a Milli-Q water purification system (Millipore, MA, USA).

## 2.2. Solutions and samples

All the oligonucleotides were diluted in 10 mM, pH 8.5 Tris-HCl buffer solution (containing 1 mM EDTA and 50 mM KCl) to give stock solutions of 10 μM. And each DNA probe was heated to 95 °C for 5

min, and slowly cooled down to room temperature. The DNA probes were then stored at 4 °C for use.

Healthy human serum samples were donated by Longhua Hospital (Shanghai) and used with the approval of the ethical committee of Shanghai Jiao Tong University. For the human serum preparation, blood samples were collected without anticoagulation reagent, stored at room temperature for two hours, then centrifuged at 1000 g for 20 min. The supernatant was taken and stored at -80 °C for use. Human breast adenocarcinoma (MCF-7) cell lysate samples were prepared by using TRIzol reagent according to the manufacturer's instructions.

### 2.3. ET method for miRNA detection

Before an ET run, an ET chip (500 μm × 500 μm × 10 mm) were fabricated (**Supplementary Information S1**) and sequentially rinsed with 100 mM NaOH solution, ultrapure water, 10 mM HCl solution and ultrapure water for 10 min each. 2% (w/v) agarose gel was then heated until complete fusion in TAE buffer solution (containing 75 mM KCl and 10 μL SGI) and filled into the channels. After that, CHA amplification was conducted in the cathode well (**Fig. 1A**). Target miRNA samples were incubated with 50 nM H1 and H2 in 10 mM, pH 8.5 Tris-HCl buffer with 1 mM EDTA and 50 mM KCl for 80 min at 38 °C. Subsequently, 20 μg/mL graphene oxide (GO) was added into the reaction solution and further incubated at 38 °C for 10 min. Then pH 6.0 TAE buffer with 75 mM KCl was added into the anode well. Next, 30 V was applied across the channel (**Fig. 1B**). At last, the movement of MRB was recorded on the CCD camera (Zhang et al., 2016) shown in **Fig. 1C**.

## 3. Results and Discussion

### 3.1. Model of miRNA ET

The model of miRNA ET bioassay is illustrated in **Fig. 1**, in which miRNA-122 is used as a model analyte and two DNA hairpin probes (H1 and H2) are ingeniously designed based on the principle of CHA. In H1, the target recognition domains (the segments of 1*, 2*, 3*) are totally complementary with the target sequence and the segments of 2*, 3*, 4, 3 are complementary to H2. In the absence of miRNA-122, the CHA process cannot be triggered. Thus, H1 and H2 can maintain the stable stem-loop structures in the cathode well and be adsorbed on GO surface due to their sticky stem region and single-stranded loop region. After use of an electric field, no DNA duplexes migrate into the ET channel, and the whole channel exhibits no fluorescence.

However, if miRNA-122 exists in the cathode well, it hybridizes with the segment 1* of H1 and unfolds

the hairpin structure of H1 via the toehold-mediated strand displacement reaction to generate the H1-target duplex. Thus, the segment 3 of H1 further hybridizes with the segment 3* of H2, leading to the yield of H1-H2 duplexes and the release of miRNA (**Fig. 1A**). The free target miRNA-122 further hybridizes with the H1 sequence and the next CHA cycle is initiated, generating numerous H1-H2 duplexes, as shown in Reaction (I).

$$\mathrm{miRNA} + \mathrm{H1} + \mathrm{H2} \xrightarrow{\Delta} \mathrm{H1\text{-}H2} + \mathrm{miRNA} \quad \text{(I)}$$

After Reaction (I), GO is added into the incubation solution, and the free H1 and H2 are closely adsorbed onto GO surface via π-stacking interaction between DNA nucleobases and GO. However, the H1-H2 duplexes are not adsorbed on GO surface due to the efficient shielding of nucleobases within the negatively charged phosphate backbone of double-stranded DNA. Thus, when an electric field is applied across the ET channel, the duplexes of H1-H2 move into the channel due to their negative charges. The free alkaline groups of H1-H2 duplexes react with the acidic TAE buffer in the channel,

$$(\mathrm{H1\text{-}H2}) + \mathrm{nH^+} \rightarrow \mathrm{H}_n(\mathrm{H1\text{-}H2}) \quad \text{(II)}$$

Reaction (II) results in an MRB between the duplexes of H1-H2 and the acidic TAE buffer. If the solution of acidic TAE buffer in the channel is termed as phase α, Reaction (II) yields phase β containing the duplexes of H1-H2 (Cao, 1998; Cao, et al., 2005),

$$(\mathrm{H1\text{-}H2})(\beta,-)||[\rightarrow]\mathrm{TAE\ buffer\ (pH\ 6.0)}(\alpha,+) \quad \text{(A)}$$

where, the symbols of "α" and "β" indicate phase $\alpha$ and β, respectively, the symbols of "+" and "−" imply the anode and cathode, respectively, the symbols of "||" and "→" are the MRB of Boundary (A) and the direction of boundary, respectively. A fluorescence indicator (SGI) is distinctly used to denote the MRB displacement in real time (**Fig. 1B**). The boundary velocity ($V_{\mathrm{MRB}}$) is computed via (Cao, 1998)

$$V_{\mathrm{MRB}} = \frac{L_2 - L_1}{t_2 - t_1} \quad (1)$$

where, $L_1$ and $L_2$ are respectively the lengths of boundary movement at the running times of $t_1$ and $t_2$. The theoretical velocity of MRB in **Fig. 1B** is obtained via

$$v_{\mathrm{MRB}} = \frac{\bar{c}_{\mathrm{H^+}}\bar{v}_{\mathrm{H^+}} - nc_{\mathrm{D}}v_{\mathrm{D}}}{\bar{c}_{\mathrm{H^+}} - nc_{\mathrm{D}}} \quad (2)$$

where, $\bar{c}_{\mathrm{H^+}}$ and $\bar{v}_{\mathrm{H^+}}$ are the constituent equivalent concentration (Equiv/L) and velocity (m/s) of hydrogen ion, respectively; $c_{\mathrm{D}}$ and $v_{\mathrm{D}}$ are the equivalent concentration (Equiv/L) and velocity (m/s) of H1-H2 duplex ion, respectively. If there is a linear relation between the fluorescence of H1-H2/SGI and the

logarithm of miRNA concentration, and the fluorescent intensity of H1-H2 is proportional to H1-H2 content, there is the following relationship between the logarithm of miRNA-122 content ($c_{\mathrm{miRNA}}$) and the MRB distance ($L_{\mathrm{MRB}}$) (**Supplementary Information S2**),

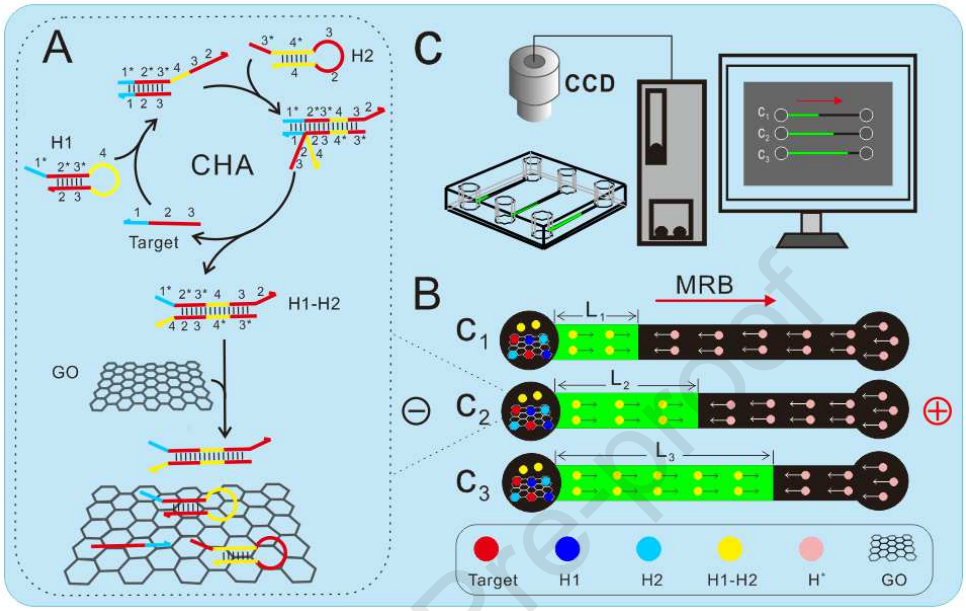


**Fig. 1**. Schematic illustration of facile thermometer-like ET biosensor for alternative miRNA assay via MRB chip (**A**), electrophoresis titration (**B**) and CCD image (**C**).

$$L_{\mathrm{MRB}} = \alpha \log c_{\mathrm{miRNA}} + \beta \qquad (3)$$

where, $\alpha$ and $\beta$ are two constants. Eq. (3) is highly simple, but shows the key relationship between the logarithmic content of target analyte and the distance of MRB movement. Evidently, Reaction (I)-(II), Boundary (A), and Eq. (1)-(3) indicate that the higher the target miRNA content in sample is, the more the H1-H2 duplex content yields, the faster MRB motion becomes, and the longer distance of MRB is within the given time (**Fig. 1B**). Hence, the target miRNA content can be visually detected with the boundary motion via the ET chip sensor of **Fig. 1**. Evidently, the thermometer-like model of ET sensing for miRNA assay is greatly facile just by reading out the MRB movement via the ET chip (**Fig. 1B-1C**).

## 3.2. Demonstration of miRNA ET Model

Herein, miRNA-122 was chosen as model analyte for proof-of-concept demonstration (**Supplementary Information S3**). **Fig. 2A** depicted the experiments of miRNA ET chip in response to 50 pM miRNA-122 with the different running times. There were clear fluorescent band movements as the miRNA ET run continuously, briefly validating Eq. (1)-(2) and the model of **Fig. 1**. **Fig. 2A** further revealed that the fluorescent band gradually expanded with the increase of running time, qualitatively validating Eq. (1)-(2),

and the model and method of **Fig. 1**.

**Fig. 2B** exhibited the boundary motions under the different running times and miRNA contents ranging from 0.02 to 1000 pM. Evidently, there were high correlation coefficients changing from 0.9973 to 0.9995, indicating good linear relations between the boundary motion and the ET time. The experiments validated Eq. (1)-(2) quantitatively. **Fig. 2B** further unveiled that the higher the miRNA-122 content was, the longer the MRB movement distance was, quantitatively validating Eq. (3) and the model and method of **Fig. 1**.

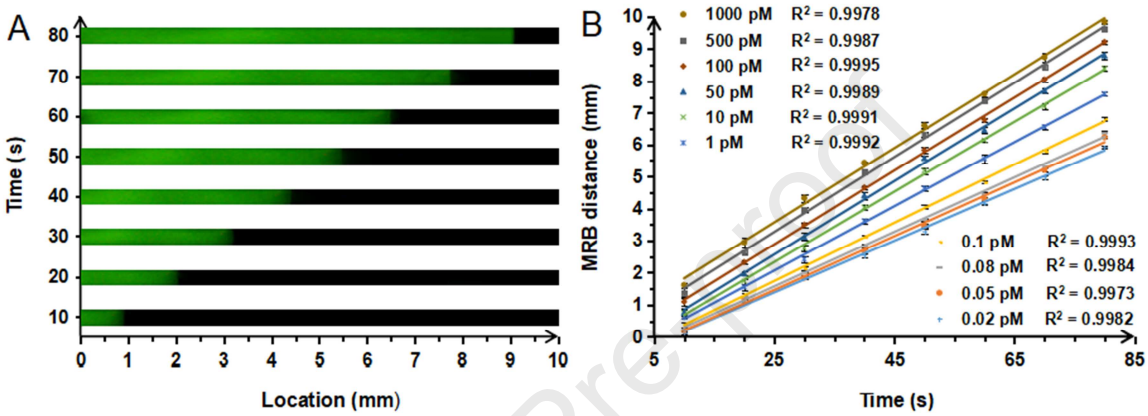


**Fig. 2**. Experiments sensing of miRNA-122 on the miRNA ET chip at different running times. (**A**) Imaging of boundary movements during the 0-80 s run of MRB created with the acidic TAE buffer (pH 6.0) and the H1-H2 duplexes yielded by CHA with 50 pM miRNA-122. (**B**) Calibration curves of MRB distance *vs*. the running time of miRNA ET under different miRNA-122 concentrations (0.02, 0.05, 0.08, 0.1, 1.0, 10, 50, 100, 500 and 1000 pM). Conditions: 10 mM, pH 8.5 Tris-HCl buffer with 1 mM EDTA and 50 mM KCl, 50 nM H1, 50 nM H2 and 20 μg/mL GO in the cathode well, incubation for 80 min at 38 °C, 2% agarose gel with 75 mM KCl, 10 μL SGI and TAE buffer in channel, 75 mM KCl and TAE buffer in the anode well, 30 V and 25 °C. The bars represented the standard deviations of three parallel runs.

The proposed ET biosensor had high facility due to the following reasons. First, the ET model and method were based on the boundary motion distance (viz., thermometer-like reading) rather than complex fluorescent intensity sensing, electrochemical biosensing and gel electrophoresis with fluorescent staining (**Table 1**), implying a facile miRNA assay. Second, Eq. (3) showed the relation between the boundary moving distance and the logarithm of miRNA-122 content, displaying the facile assay of miRNA-122. Third, **Fig. 2B** and **3** unveiled the simple assay of miRNA ET chip. Fourth, the CCD in **Fig. 1C** could be displaced with an iPhone, implying simplicity and low cost (**Fig. 1** in Cao et al., 2018).

Numerous gel electrophoresis methods have been used for the miRNA assay after isothermal amplification (Lee et al., 2014; Lee et al., 2015; Dai et al., 2018; Zhang et al., 2018). Whereas, the ones in the previous works was in nature different from the one herein. Since the ones in the previous works were

used as a separative tool for isolating target miRNA from other nucleic acids and monitoring the target within the gel via signaling fluorescence intensity, the one herein was designed for assaying the target via the reading of thermometer-like ET rather than the signaling of fluorescence intensity. To the authors' best knowledge, the thermometer-like ET biosensor was rarely reported for nucleic acid (e.g., miRNA) assay.

### 3.3. High Sensitivity of miRNA ET

To evaluate the performance of the designed miRNA ET assay, the miRNA-122 standard solutions with different concentrations were incubated with a mixture solution (containing H1, H2 and GO) and detected by the ET biosensor under the optimized conditions (**Fig. S2-S5**). **Fig. 3** displayed the experiments of miRNA ET assay under different miRNA-122 concentrations at the running times (50, 60, 70 and 80 s). Clearly, the logarithm of miRNA-122 concentration was as linear relation with the MRB distance in the miRNA content range of 20 fM to 1 nM. The correlation coefficients for the runs of 50, 60, 70 and 80 s were respectively 0.9911, 0.9914, 0.9919 and 0.9922, indicating high correlation between the MRB motion and miRNA-122 content, quantitatively validating Eq. (3) and the ET model and method.

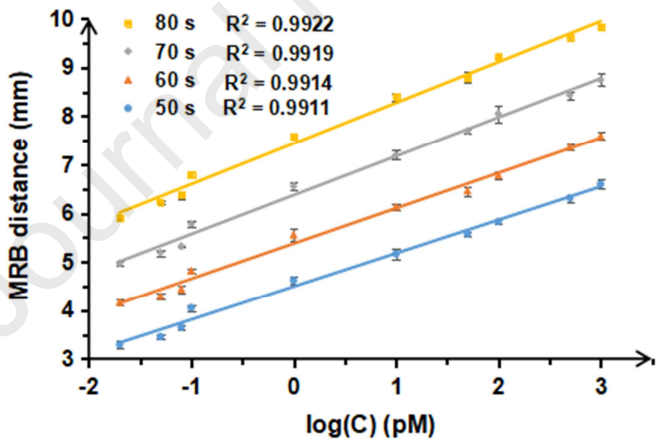


**Fig. 3**. Regression curves of MRB motion distance *vs.* the logarithm of miRNA-122 concentration (0.02, 0.05, 0.08, 0.1, 1.0, 10, 50, 100, 500 and 1000 pM) at the running times of 50, 60, 70 and 80 s. The conditions were the same as those in **Fig. 2** (n = 3). The bars represented the standard deviations of three parallel runs.

The detection of limit (LOD) of the proposed sensor was evaluated by progressively diluting the standard miRNA-122 sample until no obvious MRB movement was observed within the 80 s run of miRNA ET. The LOD for miRNA-122 was experimentally determined as 10 fM under the optimized conditions (**Supplementary Information S4**). The sensitivity of 10 fM herein was evidently poorer than the one of 0.3 fM achieved via the double amplification of HCR-CHA (Wei et al., 2016), but still indicated more than

100-fold sensitive increase in contrast to the ones with a single amplification of CHA (**Table 1**).

**Table 1**. Sensitivity comparisons of different biosensing methods with a single miRNA CHA amplification.

| Method | Linear range | LOD | Ref. |
|---|---|---|---|
| CHA-fluorescent sensing | 0.5 - 50 nM | 72 pM | Liu et al., 2017 |
| CHA-fluorescent sensing | 4.0 pM - 40 nM | 1.48 pM | Li et al., 2018 |
| CHA-fluorescent sensing | 0 - 16 nM | 47 pM | Zhen et al., 2017 |
| CHA-fluorescent sensing | 0 - 4 nM | 34 pM | Fang et al., 2018 |
| CHA-electrochemical sensing | 0 - 20 nM | 0.16 nM | Zhang et al., 2017 |
| CHA-PAGE | 50 pM - 8.0 nM | 10 pM | Zhang et al., 2018 |
| CHA-ET | 20 fM - 1.0 nM | 10 fM | This method |

The 100-fold sensitive increase of miRNA ET bioassay might be induced by the following mechanism (**Supplementary Information S5**). First, the H1-H2 duplexes yielded in CHA were electrophoresed into the ET channel and the ET assay was conducted in the channel rather than the original CHA well with the background interference of H1 and H2 as done in a normal miRNA assay. This evidently avoided the original interference of H1 and H2 in the CHA well. Second, in the model of miRNA ET, the interference of H1 and H2 was absorbed onto the surface of GO, which could not migrate into the channel during the ET progress due to molecular sieve of agarose gel used in the ET channel. This further prevented the ET bioassay from the interference of H1 and H2 originated from the cathodic well.

To unveil the mechanism on the sensitive increase of miRNA ET bioassay, a series of the comparative experiments were carried out (**Fig. S6-S8, Supplementary Information S5**). The comparisons in **Fig. S6** indicated that the fair strong interference existing in a similar CHA-based miRNA assay was greatly eliminated by the proposed method. The comparisonsin **Fig. S7** obviously unveiled that the GO added in the incubation solution of miRNA ET was not electrophoresed into the ET channel due to relatively large size of GO (~5 mm in width × 2-10 nm in thickness) in contrast to the small molecular sieve of agarose gel (average pore size of 20 nm). And the duplexes of H1-H2 but not H1 and H2 were migrated into the channel during the ET bioassay. **Fig. S8** evidently verified that H1 and H2 were absorbed onto GO and could not electrically forced into the channel if GO was added into the cathode well. However, the duplexes of H1-H2 were not absorbed by the GO and could be titrated by the acidic TAE buffer in the channel.

### 3.4. Selectivity of miRNA ET

The specificity of miRNA ET was further investigated by adding one base-, three base-mismatched

sequences of miRNA-122 (SM miRNA-122 and TM miRNA-122), four kinds of different miRNAs (miRNA-141, miRNA-21, miRNA-155 and miRNA let-7a) and a family member of miRNA-122 (miRNA-122b) into the reaction system, respectively (**Table S1**). The experiments were presented in **Fig. 4A**. Evidently, the MRB distance for SM miRNA-122, TM miRNA-122, miRNA-141, miRNA-21, miRNA-155, miRNA let-7a and miRNA-122b were much lower than the one of miRNA-122, indicating a fair selectivity of miRNA ET bioassay. The experiments of miRNA-122 ET assay with disturbance of SM miRNA-122, TM miRNA-122, miRNA-141, miRNA-21, miRNA-155, miRNA let-7a and miRNA-122b were carried out for testing the selectivity of the ET method. As shown in **Fig. 4B**, all the interfering miRNAs had no remarkable influence on the MRB movement in miRNA-122 ET assay. **Fig. 4A-4B** evidently manifested that the proposed strategy exhibited good specificity for clearly discriminating miRNA-122 from other mismatched sequences and miRNAs, even single-nucleotide mismatch.

The high selectivity attributed to the following reasons. First, the CHA in miRNA ET bioassay was specifically triggered by the miRNA-122, which was critically based on the perfect match between the miRNA-122 and DNA hairpin probes. Second, there were different affinities of GO to various DNA probes, improving the selectivity of miRNA-122 ET assay. Third, molecular sieve of agarose gel existed to GO with interference of H1, H2 and mismatched sequences, further enhancing the selectivity of miRNA ET. All these implied that the ET had the potential to assay target miRNA in complex bio-samples.

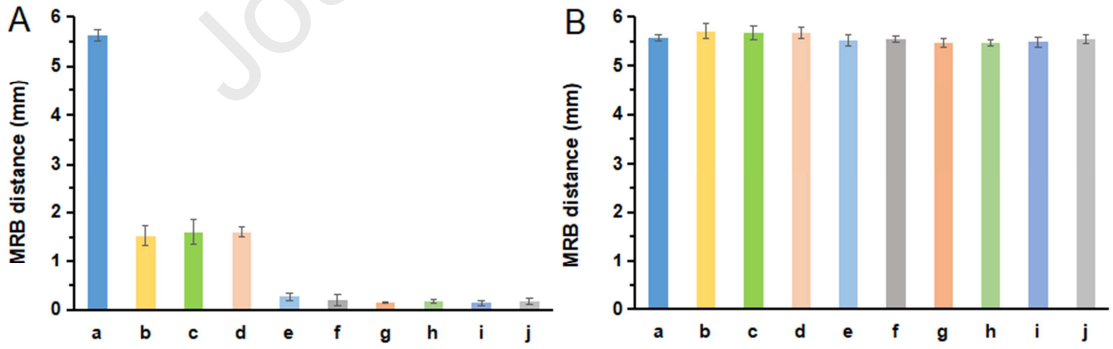


**Fig. 4**. (**A**) Selectivity of the ET system to target miRNA-122. The boundary motion distances at 50 s run of MRB with 50 pM miRNA-122 (**a**), SM miRNA-122-L (**b**), SM miRNA-122-M (**c**), SM miRNA-122-R (**d**), TM miRNA-122 (**e**), miRNA-141 (**f**), miRNA-21 (**g**), miRNA-155 (**h**), miRNA let-7a (**i**) and miRNA-122b (**j**). (**B**) Experiments of miRNA ET assay with disturbance of 50 pM SM miRNA-122-L (**b**), SM miRNA-122-M (**c**), SM miRNA-122-R (**d**), TM miRNA-122 (**e**), miRNA-141 (**f**), miRNA-21 (**g**), miRNA-155 (**h**), miRNA let-7a (**i**) and miRNA-122b (**j**) in 50 pM miRNA-122 (**a**) solution. The conditions were the same as those in **Fig. 2** (n = 3). The bars were the standard deviations of three parallel runs.

### 3.5. Stability of miRNA ET

The stability of the proposed biosensing system was statistically evaluated by analysing the relative standard deviations (RSDs) of intra-day and inter-day experiments (**Supplementary Information S6**). A series of miRNA-122 samples with different concentration levels (5, 10 and 20 pM) were determined by the proposed method with three repetitive measurements. **Table S2** revealed that the RSD values of intra-day and inter-day experiments were 2.01%-3.03% and 2.28%-4.01%, respectively, implying quite good stability of the developed method.

### 3.6. Reliability and application of miRNA ET

The analytical reliability of the ET biosensing was evaluated via recovery experiments. In the runs, healthy human serum and MCF-7 cell lysate samples were spiked with miRNA-122 at different levels (5, 10 and 20 pM) and then determined by the proposed method with three repetitive runs (**Table S3**). The recoveries of human serum were from 96.2% to 102% and the RSD values were 1.07%-6.25%. And the recoveries of MCF-7 cell lysate were from 97.9% to 110% and the RSDs were 2.88%-7.32%. All data in **Table S3** implied that the ET sensing exhibited quite good accuracy and anti-interference. Evidently, the recovery experiments of miRNA let-7a further certified the good accuracy of the model and method of ET sensing (see **Table S4**).

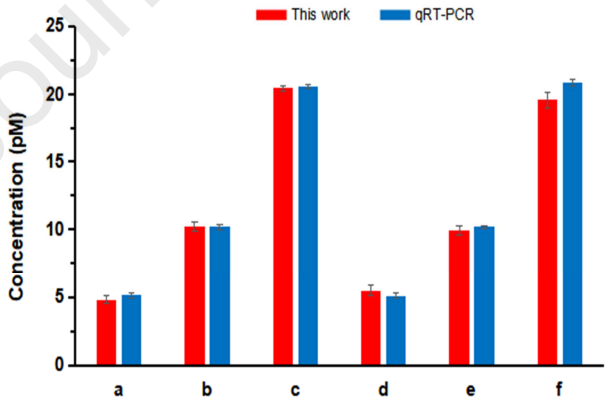


**Fig. 5**. Comparative assays of miRNA-122 content in spiked healthy human serum and MCF-7 cell lysate via miRNA ET and qRT-PCR. The distances of boundary motion at 50 s ET run with miRNA-122 in serum (**a**: 5 pM; **b**: 10 pM; **c**: 20 pM) and MCF-7 cell lysate (**d**: 5 pM; **e**: 10 pM; **f**: 20 pM). The conditions were the same as those in **Fig. 2** (n = 3). The bars represented the standard deviations of three parallel runs.

**Fig. 5** displayed the comparative experiments and relevant statistical data on the serum and MCF-7 cell lysate samples spiked with miRNA-122 and assayed with both the miRNA ET and standard qRT-PCR. The comparative experiments in **Fig. 5** revealed that the quantitation results obtained via the proposed ET method were in good agreement with the ones detected via the standard method of qRT-PCR, indicating the

validity of developed ET sensing. All these indicated that the miRNA ET method had a good reliability for complex samples assay, and had evident potential for real application of clinical bioassay.

## 4. Conclusions

In summary, a facile thermometer-like model of electrophoresis titration (ET) biosensor was proposed for sensitive miRNA assay via an MRB chip. The ET model unveiled that the MRB distance was as a function of logarithm of miRNA-122 content implying a facile thermometer-like biosensing model. The systemic experiments were carried out and validated the facile model and method of miRNA ET. Benefiting from the efficient CHA and the elimination of background signal interference via MRB and GO, the proposed miRNA ET also had high sensitivity and specificity. Furthermore, the developed method had good stability, accuracy and reliability. Finally, the presented method was applied for the real bioassay of miRNA-122 and miRNA let 7a in human serum and cancer cell lysate. Of course, the developed miRNA ET method still suffered from some drawbacks. For example, the LOD of ET method (10 fM) was poorer than the one with multiple amplification (0.3 fM, Wei et al., 2016), and currently the power supply and CCD with large scale volume were used for the ET experiments indicating the difficulty of portable miRNA ET device. Thus, further effort has to be given for improving the sensitivity and portability of miRNA ET method via multiple amplification and lithium battery as well as a smart phone camera (Cao, et al., 2018). Such a research was under its course.

### Credit authorship contribution statement

**Ling Chen:** Conceptualization, Data curation, Formal analysis, Investigation, Methodology, Draft organization. **Qiang Zhang:** Methodology, Writing - review & editing. **Weiwen Liu:** Writing - review & editing. **Hua Xiao:** Resources. **Xiaoping Liu:** chip design & fabrication. **Liuyin Fan:** Validation. **Yuxing Wang:** Validation. **Honggen Li:** Device, Validation, Funding asistance. **Chengxi Cao:** Conceptualization, Funding acquisition, Investigation, Methodology, Project administration, Writing-review & editing.

### Declaration of competing interest.

The authors declare that they have no known competing financial interests or personal relationships that could have appeared to influence the work reported in this paper.

**Acknowledgements.** Great appreciation is expressed to Chun-Hui Huo for his preparation on the serum sample. This work was supported by grants from the National Natural Science Foundation of China (No.

31727801 and 21605101).

## References


Ahmed, C.S., Winlow, P.L., Parsons, A.L., Jopling, C.L., 2018. Nucleic Acids Res. 46, 6330-6343.

Bartel, D.P., 2009. Cell 136, 215-233.

Bhattacharya, A., Leprohon, P., Bigot, S., Padmanabhan, P.K., Mukherje, A., Roy, G., Gingras, H., Mestdagh, A., Papadopoulo, B., Ouellette, M., 2019. Nat. Commun. 10, 5627.

Brase, J.C., Wuttig, D., Kuner, R., Sultmann, H., 2010. Mol. Cancer 9, 306.

Cao, C.X., 1998. J. Chromatogr. A 813, 153-171.

Cao, C.X., Zhang, W., Qin, W.H., Li, S., Liu, W., 2005. Anal. Chem. 77, 995-963.

Cao, X.Y., Kong, F.Z., Zhang, Q., Liu, W.W., Liu, X.P., Li, G.Q., Zhong, R., Fan, L.Y., Xiao, H., Cao, C.X., 2018. Lab Chip 18, 1758-1766.

Chen, J.H., Zhou, X.M., Zeng, L.W., 2013. Chem. Commun. 49, 984-986.

Dai, W.H., Zhang, J., Meng, X.D., He, J., Zhang, K., Cao, Y., Wang, D.D., Dong, H.F., Zhang, X.J., 2018. Theranostics 8, 2646-2656.

Deman, J., 1970. Anal. Chem. 42, 1699-1705.

Deman, J., 1970. Anal. Chem. 42, 983-989.

Ding, L.H., Liu, H.Y., Zhang, L.N., Li, L., Yu, J.H., 2018. Sensor. Actuator. B 254, 370-376.

Fang, H.M., Xie, N.L., Ou, M., Huang, J., Li, W.S., Wang, Q., Liu, J.B., Yang, X.H., Wang, K.M., 2018. Anal. Chem. 90, 7164-7170.

Ge, J., Zhang, L.L., Liu, S.J., Yu, R.Q., Chu, X., 2014. Anal. Chem. 86, 1808-1815.

Ha, M., Kim, V.N., 2014. Nat. Rev. Mol. Cell Biol. 15, 509-524.

He, L., Thomson, J.M., Hemann, M.T., Hernandomonge, E., Mu, D., Goodson, S., Powers, S., Cordon-Cardo, C., Lowe, S.W., Hannon, G.J., Hammond, S.M., 2005. Nature 435, 828-833.

Howell, L.S., Ireland, L., Park, B.K., Goldring, C.E., 2018. Expert Rev. Mol. Diagn. 18, 47-54.

Huang, J.H., Su, X.F., Li, Z.G., 2012. Anal. Chem. 84, 5939-5943.

Hwang, H.W., Mendell, J.T., 2006. Br. J. Cancer 94, 776-780.

Kawasaki, H., Taira, K., 2003. Nature 423, 838-842.

Kong, F.Z., Jahan, S., Zhong, R., Cao, X.Y., Li, W.L., Wang, Y.X., Xiao, H., Liu, W.W., Cao, C.X., 2019. ACS Sens. 4, 1126-133.

Lee, H., Srinivas, R.L., Gupta, A., Doyle, P.S., 2015. Angew. Chem. Int. Ed. 54, 2477-2481.

Lee, H.J., Park, J.E., Nam, J.M., 2014. Nat. Commun. 5, 3367.

Lee, J.M., Cho, H., Jung, Y.W., 2010. Angew. Chem. Int. Ed. 49, 8662-8665.

Li, J., Yao, B., Huang, H., Wang, Z., Sun, C.H., Fan, Y., Chang, Q., Li, S.L., Wang, X., Xi, J.Z., 2009. Anal. Chem. 81, 5446-5451.

Li, S., Xu, L.G., Ma, W., Wu, X.L., Sun, M.Z., Kuang, H., Wang, L.B., Kotov, N.A., Xu, C.L., 2016. J. Am. Chem. Soc. 138, 306-312.

Li, S.Y., Liu, C., Gong, H., Chen, C.Y., Chen, X.M., Cai, C.Q., 2018. Talanta 178, 974-979.

Li, X.M., Cheng, W., Li, D.D., Wu, J.L., Ding, X.J., Cheng, Q., Ding, S.J., 2016. Biosens. Bioelectron. 80, 98-104.

Liao, M.F., Hsu, J.L., Lu, K.T., Chao, P.K., Cheng, M.Y., Hsu, H.C., Lo, A.L., Lee, Y.L., Hung, Y.H., Lyu, R.K., Kuo, H.C., Chu, C.C., Ro, L.S., 2020. Cell 9, 1669.

Liu, S.F., Wang, Y., Ming, J.J., Lin, Y., Cheng, C.B., Li, F., 2013. Biosens. Bioelectron. 49, 472-477.

Liu, Y., Shen, T., Li, J., Gong, H., Chen, C.Y., Chen, X.M., Cai, C.Q., 2017. ACS Sens. 2, 1430-1434.

Mariana, L.Q., Reinhard, R., Abdullah, Y., Jutta, M., Winfried, L., Thomas, T., 2002. Cur. Biol. 12, 735-739.

Necsulea, A., Soumillon, M., Warnefors, M., Liechti, A., Daish, T., Zeller, U., Baker, J.C., Grützner, F., Kaessmann, H., 2014. Nature 505, 635-640.

379 Nicoloso, M.S., Spizzo, R., Shimizu, M., Rossi, S., Calin, G.A., 2009. Nat. Rev. Cancer 9, 293-302.
380 Pall, G.S., Codony-Servat, C., Byrne, J., Ritchie, L., Hamilton, A., 2007. Nucleic Acids Res. 35, e60.
381 Rafiee-Pour, H.A., Behpour, M., Keshavarz, M., 2016. Biosens. Bioelectron. 77, 202-207.
382 Tao, S., Liu, Y.B., Zhou, Z.W., Lian, B., Li, H., Li, J.P., Zhou, S., 2016. Am. J. Transl. Res. 8, 1659-1677.
383 Ventura, A., Jacks, T., 2009. Cell 136, 586-591.
384 Wang, C.H., Zhang, Q., Liu, X.P., Li, G.Q., Kong, H., Khan, M.I., Xiao, H., Wang, Y.X., Liu, W.W., Cao,
385 C.X., 2019. Lab Chip 19, 484-492.
386 Wei, Y.L., Zhou, W.J., Li, X., Chai, Y.Q., Yuan, R., Xiang, Y., 2016. Biosens. Bioelectron. 77, 416-420.
387 Wen, Y.Q., Xu, Y., Mao, X.H., Wei, Y.L., Song, H.Y., Chen, N., Huang, Q., Fan, C.H., Li, D., 2012. Anal.
388 Chem. 84, 7664-7669.
389 Xiao, C.C., Rajewsky, K., 2009. Cell 136, 26-36.
390 Yang, C.Y., Shi, K., Dou, B.T., Xiang, Y., Chai, Y.Q., Yuan, R., 2015. ACS Appl. Mater. Inter. 7,
391 1188-1193.
392 Yu, Y.Y., Chen, Z.G., Shi, L.J., Yang, F., Pan, J., Zhang, J.B., Sun, D.P., 2014. Anal. Chem. 86,
393 8200-8205.
394 Zhang, H., Wang, Q., Yang, X.H., Wang, K.M., Li, Qi., Li, Z.P., Gao, L., Nie, W.Y., Zheng, Y., 2017.
395 Analyst 142, 389-396.
396 Zhang, J.Q., Zhang, W.C., Gu, Y.Q., 2018. Anal. Biochem. 550, 117-122.
397 Zhang, K., Wang, K., Zhu, X., Xu, F., Xie, M.H., 2017. Biosens. Bioelectron. 87, 358-364.
398 Zhang, L.X., Cao, Y.R., Xiao, H., Liu, X.P., Liu, S.R., Meng, Q.H., Fan, L.Y., Cao, C.X., 2016. Biosens.
399 Bioelectron. 77, 284-291.
400 Zhen, S.J., Xiao, X., Li, C.H., Huang, C.Z., 2017. Anal. Chem. 89, 8766-8771.
401 Zhong, J.F., He, Y., Chen, W.J., Shui, X.R., Chen, C., Lei, W., 2014. Int. J. Mol. Sci. 15, 20355-20364.
402 Zhu, H.L., Luo, H., Zuo, X.X., 2013. Exp. Mol. Med. 45, e41.

- A thermometer-like model of miRNA ET biosensor via MRB chip
- Sensitivity increase of ET assay by interference elimination via MRB and GO
- High simplicity, sensitivity, specificity and stability of miRNA ET assay
- Real use of ET sensor to assay of miRNA in serum and cancer cell lysate

**Declaration of interests**

☒ The authors declare that they have no known competing financial interests or personal relationships that could have appeared to influence the work reported in this paper.

☐The authors declare the following financial interests/personal relationships which may be considered as potential competing interests: